

Evaluation of Liver Masses and Accompanying Findings by Diffusion-Weighted Magnetic Resonance Imaging

Ümmü Gülsüm Özgül Gümüş¹, Ökkeş İbrahim Karahan²

¹Department of Pediatric Radiology, Erciyes University, Faculty of Medicine, Kayseri, Turkey

²Department of Radiology, Erciyes University, Faculty of Medicine, Kayseri, Turkey

ABSTRACT

Objective: The aim of this study was to investigate the contribution of diffusion-weighted magnetic resonance imaging to differential diagnosis in the characterization of liver masses.

Methods: Diffusion-weighted sequences were added to conventional sequences in cases in which a mass was detected during upper abdominal magnetic resonance imaging performed for any reason. Diffusion-weighted images were obtained by applying diffusion-sensitive gradients at the b0, b600, and b1000 values with a single shot echo-planar spin echo sequence in the axial plane using the 1.5T magnetic resonance imaging device, and apparent diffusion coefficient maps were automatically constructed from these images by the magnetic resonance imaging device. The mean apparent diffusion coefficient values were calculated for 56 masses and 45 liver parenchyma in 45 cases with histopathological diagnoses.

Results: Of the 56 masses, 28 were benign and 28 were malignant. The benign masses consisted of 11 hemangiomas, 8 hydatid cysts, 3 simple cysts, 4 abscesses, and 2 focal nodular hyperplasia. The malignant masses comprised 13 hepatocellular carcinomas, 12 metastases, 2 cholangio cellular carcinomas, and 1 carcinosarcoma. The mean apparent diffusion coefficient value of the benign masses was calculated to be 2.67×10^{-3} s/mm² and that of the apparent diffusion coefficient value was 1.21×10^{-3} s/mm², indicating a statistically significant difference between the 2 groups. Apparent diffusion coefficient combined with diffusion-weighted magnetic resonance imaging had 100% sensitivity and 69% specificity in the differentiation of benign and malignant masses.

Conclusion: Diffusion-weighted magnetic resonance imaging is a technique that provides results in a short time without using any contrast agent and contributes to the differential diagnosis of liver masses and should be added to conventional sequences.

Keywords: Hepatic masses, diffusion-weighted imaging, magnetic resonance imaging, cyst hydatid, hepatic hemangioma

INTRODUCTION

The liver is an organ in which benign and malignant lesions are frequently located.¹ The characterization of focal mass lesions in the liver can be performed with high accuracy (97%) using T1-weighted, T2-weighted, and dynamic contrast-enhanced examinations and fat-suppressed sequences in routine liver examination by magnetic resonance imaging (MRI).²

Diffusion refers to the random motion of molecules with their kinetic energy, which is also called Brownian motion.³ Diffusion-weighted imaging (DWI) is one of the functional MRI techniques sensitive to the Brownian motion of molecules. Image contrast depends on the microscopic movements of water molecules. Images are obtained without contrast in a short exposure time. The disadvantage of this technique is that it is sensitive to magnetic field inhomogeneity, images of low geometric resolution, and low signal/noise ratio. Diffusion-weighted imaging shows significant sensitivity to current and motion.⁴

In DWI, images are T2-weighted, and apparent diffusion coefficient (ADC) maps are constructed in which only diffusion effect is seen to eliminate the T2 effect.³ An ADC map comprises synthetic images created by processing the data obtained at the pixel base to prevent T2 shine-through. The resulting images are independent of the direction of diffusion and the T2 effect. In restricted diffusion, low ADC values, that is low signal, are observed, while high ADC values are observed in increased diffusion due to high signal. As the gradient intensity (b value) used in diffusion measurement increases, phase distribution and signal loss in mobile protons also increase.⁴

The main objective of this study was to determine the DWI findings of various liver masses and investigate their contribution to diagnosis in terms of benign and malignant differentiation by calculating the characteristic features and ADC values that may be useful in the differential diagnosis.

Cite this article as: Özgül Gümüş ÜG, Karahan Öİ. Evaluation of liver masses and accompanying findings by diffusion-weighted magnetic resonance imaging. *Eur J Ther.* 2022;28(2):89–95.

Corresponding author: Ümmü Gülsüm Özgül Gümüş, e-mail: drugulsumgumus43@gmail.com

Received: November 23, 2021 **Accepted:** May 18, 2022



Copyright@Author(s) – Available online at eurjther.com.

Content of this journal is licensed under a Creative Commons Attribution-NonCommercial 4.0 International License.

METHODS

After the decision of the ethics committee of Erciyes University Faculty of Medicine (09/130, Kayseri) was taken, DWI was added to patients with liver mass detected in abdominal MRI for any reason between March 2009 and January 2010 in our hospital. Between the specified dates, liver masses were detected in 128 cases in the upper abdominal MRI. Twelve patients who could not hold their breath for any reason, 32 with masses smaller than 1 cm, and 39 without histopathological diagnoses were excluded from the evaluation. Fifty-six masses of the remaining 45 cases (26 men and 19 women) with histopathological diagnoses were examined. The age of the patients varied between 26 and 80 years, and the mean age was 59.3 ± 15.6 years.

Routine upper abdominal MRI was performed on the patients using a 1.5 Tesla MRI device (Philips Gyroscan Intera, Best, the Netherlands) with 4 phased-array coils. Before injecting the contrast agent, DWI were obtained in the single-shot echo-planar sequence in the axial plane at different b values (b0, b600, and b1000 s/mm²) [TR (Time to Repetation), 3656 ms; TE (Time to Echo), 89 ms (b1000); TR, 2673; TE, 60 (b600); matrix, 128 × 256; FOV (Field-of-view), 35-40 cm; section thickness, 7 mm; cross-section, 1 mm). Oil pressure pulses were used to prevent serious chemical-shift artifacts. The ADC maps of isotropic images were created automatically by the device.

Apparent diffusion coefficient values were calculated by placing the regions of interest (ROI) on the lesions to cover 2/3 of the area. In large lesions, measurements were taken by placing ROI at the locations corresponding to the contrasted areas of the lesions. The histopathological diagnoses of the patients were compared with the mean ADC values measured. In addition, 1 cm² ROI was placed in the liver parenchyma to calculate the ADC value of this tissue.

Statistical Package for the Social Sciences 15.0 for Windows program (SPSS Inc, Chicago, Ill, USA) was used for statistical evaluation. Quantitative data were defined as mean ± standard deviation. The difference between the 2 groups was analyzed using the Student's t test. Countable data (qualitative) were defined as a percentage. Diagnosis the sensitivity and specificity of the criteria were calculated. Kappa match between 2 tests was analyzed using statistics and the difference between them was determined by using the Mc Nemar test. The significance level was taken as .05.

Main Points

- Many benign and malignant masses may be seen in the liver.
- Diffusion-weighted images are a magnetic resonance imaging (MRI) sequence that was obtained without contrast in a short exposure time.
- Benign and malignant differentiation of liver masses can be done by diffusion-weighted magnetic resonance imaging sequence.

RESULTS

Fifty-six masses of 45 cases with histopathological diagnoses were evaluated. Of these masses, 28 were benign and 28 were malignant. The benign masses consisted of 11 hemangiomas, 8 hydatid cysts, 3 simple cysts, 4 abscesses, and 2 focal nodular hyperplasia (FNH). The malignant masses comprised 13 hepatocellular carcinomas (HCCs), 12 metastases, 2 cholangiocellular carcinomas, and 1 carcinosarcoma. The size of the benign masses ranged from 2 to 13 cm with a mean value of 7.36 ± 2.70 cm, and the size of the malignant masses varied between 1.5 and 20 cm, with a mean value of 7.55 ± 4.42 cm (Table 1).

In the quantitative evaluation of the lesions, the mean ADC measurements were obtained from the ADC maps of the b600 and b1000 images. The ADC values of 28 benign masses varied between 4.29 and 1.28×10^{-3} s/mm², with the mean value of $2.93 \pm 0.29 \times 10^{-3}$ s/mm², and the highest ADC in the benign group was observed in simple cysts with a mean value of 4.29×10^{-3} s/mm² and the lowest ADC in abscesses with a mean ADC value was measured as 1.28×10^{-3} s/mm². Among the 28 malignant masses, the ADC values ranged from 1.42 to 1.17×10^{-3} s/mm², with a mean value of $1.24 \pm 0.24 \times 10^{-3}$ s/mm². The mean ADC values of the liver parenchyma and cirrhotic livers were $1.54 \pm 0.2 \times 10^{-3}$ s/mm² and $1.43 \pm 0.4 \times 10^{-3}$ s/mm², respectively. The difference between these 2 groups (normal liver parenchyma and cirrhotic liver) was statistically significant (Table 2). There was a statistically significant difference between the mean ADC values of the benign and malignant masses (Table 3).

The hydatid cysts (n=8) showed loss of signal as the b value increased in DWI, but they were only slightly more hyperintense at the b1000 value compared to the simple cysts (Figure 1). For the hemangiomas (n= 11), hydatid cysts (n=8), and simple cysts (n=3), the ADC appearance presented with a higher value compared to the liver, while the malignant lesions except for hypovascular metastases (n= 17) and the benign lesions of abscesses (n=4) and FNH (n=2) had lower values than the liver in ADC maps

Table 1. Number and Size of Lesions According to the Lesion Type

	Number of Lesions	Lesion Size (cm)
Hemangioma	11	2-11
Hydatid cyst	8	5-13
Simple cyst	3	3-6
Abscess	4	5-9
FNH	3	3-4.5
HCC	13	2.5-15
Metastasis	12	1.5-20
CCC	2	9-10
Carcinosarcoma	1	20

FNH, focal nodular hyperplasia; HCC, hepatocellular carcinomas; CCC, cholangiocellular carcinomas.

Table 2. Mean ADC Values at b600 and b1000 According to the Lesion Type

Lesion Type	ADC 600 ($\times 10^{-3}$ s/ mm ²)	ADC 1000 ($\times 10^{-3}$ s/ mm ²)	P
Hemangioma (n = 11)	2.99 ± 0.17	2.75 ± 0.31	.43
Hydatid cyst (n = 8)	4.27 ± 0.17	3.71 ± 0.51	.07
Simple cyst (n = 3)	4.29 ± 0.18	4.09 ± 0.41	.40
Abscess (n = 4)	1.28 ± 0.59	1.21 ± 0.69	.52
FNH (n = 2)	1.32 ± 0.06	1.25 ± 0.02	.33
HCC (n = 13)	1.28 ± 0.10	1.12 ± 0.11	.50
Metastasis (n = 12)	1.17 ± 0.10	1.05 ± 0.91	.54
CCC (n = 2)	1.42 ± 0.11	1.30 ± 0.48	.38
Carcinosarcoma (n = 1)	1.27	1.11	
Normal liver (n = 38)	1.54 ± 0.2	1.41 ± 0.3	.44
Cirrhotic liver (n = 7)	1.43 ± 0.4	1.37 ± 0.5	.32

FNH, focal nodular hyperplasia; HCC, hepatocellular carcinomas; CCC, cholangiocellular carcinomas ADC, apparent diffusion coefficient.

(Figure 2). The hypovascular metastases (n = 11) had peripheral hyperintensity and central hypointensity on DWI and low peripheral and high central values in ADC maps (diffusion restriction in the peripheral area) (Figure 3). The hypervascular metastasis (n = 1), on the other hand, was observed to have homogeneous hyperintensity on DWI and a low value in ADC maps (Figure 4). The periphery of the abscesses (n = 4), especially the capsule, was iso-hypointense in DWI and had a high value in ADC maps. A significant diffusion restriction was observed in the central of the abscesses, which were observed to have hyperintensity on DWI and a low value (diffusion restriction in the central area) in ADC maps (Figure 5). Focal nodular hyperplasia (n = 3) showed hyperintensity in DWI and a low value (diffusion restriction) on ADC maps, which could be confused with malignant masses (Figure 6).

DISCUSSION

Diffusion describes the random motion of water molecules, which is also called Brownian motion.³ The amount of diffusion is determined by the diffusion coefficient. The measurement of the diffusion coefficient is affected by many factors in biological tissues, including capillary perfusion, temperature, magnetic sensitivity in tissue, and movement. Therefore, ADC maps are used instead of the diffusion coefficient.³ Diffusion-weighted imaging is important due to its rapid examination time (20-30 seconds)

Table 3. Mean ADC Values of the Benign and Malignant Masses

Masses (n = 56)	ADC 600 ($\times 10^{-3}$ s/mm ²)	ADC 1000 ($\times 10^{-3}$ s/mm ²)	P
Benign (n = 28)	2.93 ± 0.29	2.68 ± 0.26	>.05
Malign (n = 28)	1.24 ± 0.24	1.10 ± 0.72	>.05
P	<.05	<.05	

ADC, apparent diffusion coefficient.

and no requirement of contrast material.⁵ The disadvantage of this technique is that SGN is low, and therefore problems occur in the evaluation of lesions smaller than 1 cm.⁶

The most suitable b values for tissue characterization in the liver have been reported as b0 and b500-600 s/mm².⁷ When we evaluated the image quality in our study, we observed that the images obtained at b600 were higher quality and contained fewer artifacts than those obtained at b1000 values.

Diffusion-weighted images have been found to be highly sensitive and specific in the characterization of focal liver masses and diffuse liver diseases.^{6,8-10} In the literature, the mean ADC value of benign liver masses ranges from 2.45 to 1.94 s/mm², while that of malignant varies between 10.8 and 1.04 s/mm². This difference between the ADC values of the malignant and benign masses has been attributed to the former containing more cells than the latter.^{6,10} However, abscesses, FNH, adenomas (benign lesions with high cell density), and cystic necrotic tumors (malignant lesions with low cell density) are exceptions to this rule.^{7,11} In the current study, the mean ADC values of the benign and malignant masses were found to be $2.93 \pm 0.29 \times 10^{-3}$ s/mm² and $1.24 \pm 0.24 \times 10^{-3}$ s/mm², respectively, and the difference between the ADC values of these 2 groups was statistically significant, consistent with the literature. The numerical differences between ADC values in different studies are due to the changes in these values according to the b parameter, device and imaging protocol used, gradient changes, and the shooting technique.¹²

In cases where fatty liver, fibrosis, and accumulation of collagen deposit in the liver, a decrease is observed in the ADC value of the liver parenchyma.¹³ In the literature, the mean ADC value of normal liver parenchyma ranges between 0.69×10^{-3} s/mm²¹⁰ and 1.83×10^{-3} s/mm²,⁶ while the ADC value of cirrhotic liver parenchyma has been measured as 0.60×10^{-3} s/mm² and 1.37×10^{-3} s/mm², respectively, in the same studies. In the current study, the mean ADC value of normal liver parenchyma was determined as $1.54 \pm 0.2 \times 10^{-3}$ s/mm² and that of cirrhotic liver parenchyma was $1.43 \pm 0.4 \times 10^{-3}$ s/mm², indicating a statistically significant difference, which is in agreement with the literature.

In the literature, the mean ADC values of hemangiomas have been reported to vary between 2.95 and 1.92×10^{-3} s/mm², which is higher compared to malignant lesions and liver parenchyma and lower compared to cysts.^{6,10,14} In our study, we determined the mean ADC value of the hemangiomas as $2.99 \pm 0.17 \times 10^{-3}$ s/mm².

In the literature, the mean ADC values of simple cysts range from 3.63 to 2.91×10^{-3} s/mm², which is reported to be higher than those of liver masses.^{6,10,14} In the current study, we calculated the ADC value of the simple cysts as $4.29 \pm 0.18 \times 10^{-3}$ s/mm².

In a study conducted by İnan et al.,¹⁵ hydatid cysts and simple cysts were examined at b500 and b1000 on DWI, and it was reported that both groups were hyperintense compared to the liver parenchyma at b500 (T2 shine-through effect), while at b1000, hydatid cysts were minimally hyperintense and simple cysts became isointense compared to the liver parenchyma.

Figure 1. A 49-year-old patient with a hydatid cyst. On diffusion-weighted images obtained at b600, the hydatid cyst localized in segment 8 is observed as hyperintense, which is similar to simple cysts, while at b1000, it shows moderate hyperintensity to the liver unlike simple cysts.

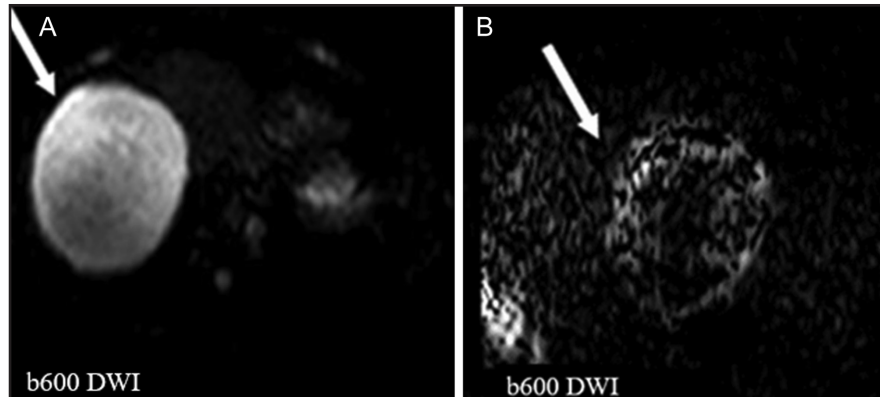


Figure 2. ADC appearance of a hydatid cyst (A), hemangioma (B), and hypervascular metastatic lesion (C). While the hydatid cyst and hemangioma are observed to have high values, the metastatic lesion has a low value. ADC, apparent diffusion coefficient.

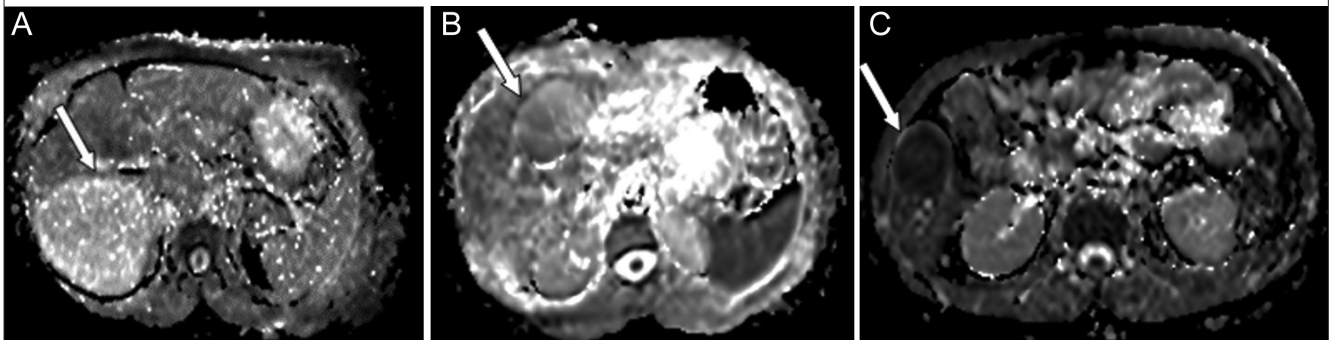
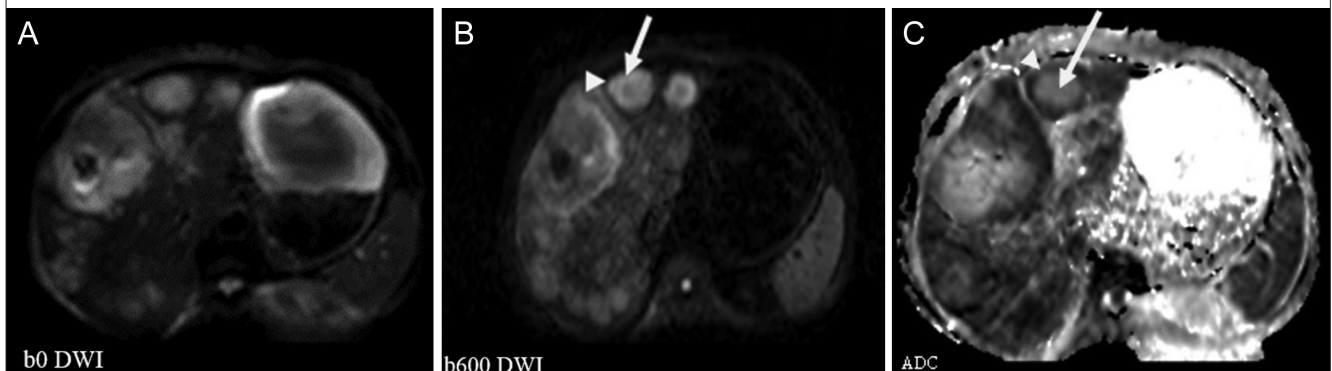


Figure 3. A 68-year-old patient with a gastric adenocarcinoma. There are numerous metastatic lesions in the liver. On DWI, the center of the lesion is hypointense (arrow) and the periphery is hyperintense (arrowhead). In the ADC map, the center has a high value (arrow) and the periphery has a low value (arrowhead). ADC, apparent diffusion coefficient; DWI, diffusion-weighted imaging.



Therefore, the authors reported that the b1000 values provided significant results. In the same study, the mean ADC value was 3.5×10^{-3} s/mm² for simple cysts and 2.9×10^{-3} s/mm² for hydatid cysts, with a statistically significant difference between the 2 groups. The authors attributed this finding to hydatid cysts

being more dense than simple cysts due to their scolex, protein, glucose, lipid, and polysaccharide content. In our study, in cases with 7 hydatid cysts and 3 simple cysts, the hydatid cysts were observed to be iso-hyperintense, while the simple cysts were isointense compared to the liver at b1000. The mean

Figure 4. A 57-year-old patient with a pancreatic neuroendocrine tumor. Liver metastasis is observed. Hypervascular metastases show homogeneous hyperintensity in diffusion-weighted images and a low value in the ADC map. ADC, apparent diffusion coefficient.

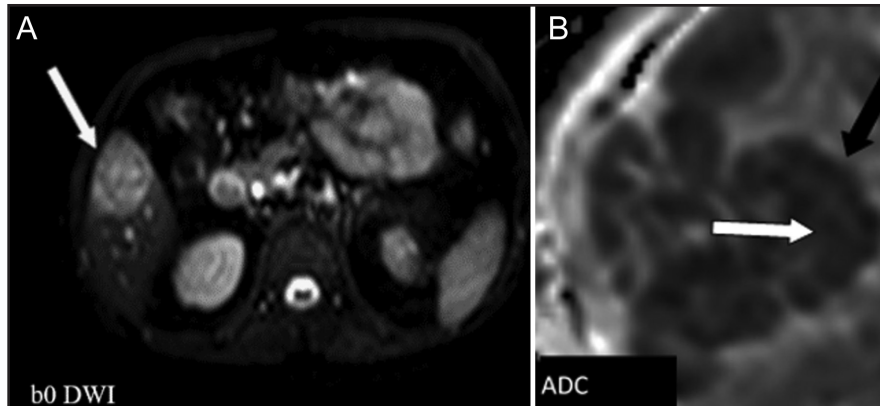


Figure 5. The abscess capsule is hypointense and the center is hyperintense on DWI. In the ADC map, the abscess capsule has a high value and the center has a low value. ADC, apparent diffusion coefficient; DWI, diffusion-weighted imaging.

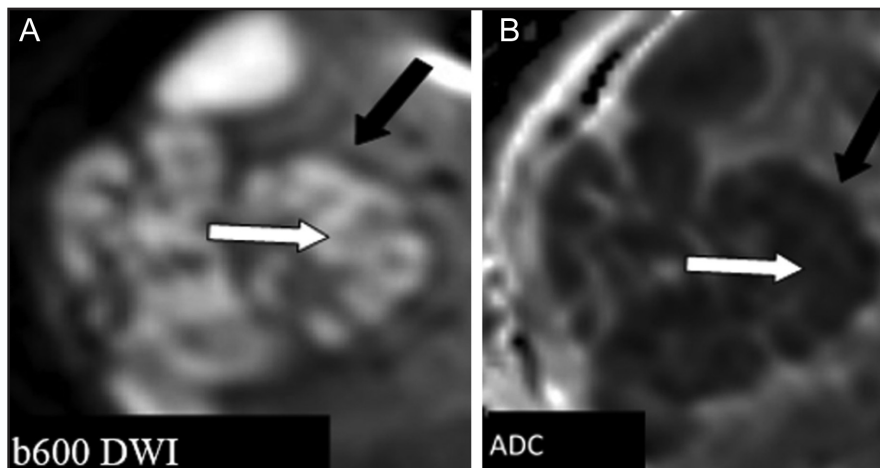
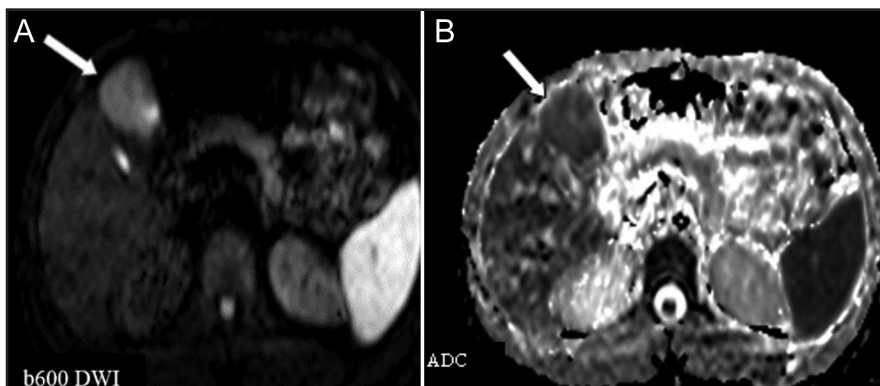


Figure 6. A 31-year-old female patient with a liver mass detected during a routine examination and diagnosed as FNH as a result of biopsy. The lesion is hyperintense on DWI and has a low value in the ADC map. ADC, apparent diffusion coefficient; DWI, diffusion-weighted imaging; FNH, focal nodular hyperplasia.



ADC values were calculated as $4.27 \pm 0.17 \times 10^{-3}$ s/mm² and $4.29 \pm 0.18 \times 10^{-3}$ s/mm² for the hydatid and simple cysts, respectively, but a statistical analysis could not be undertaken due to the insufficient number of cases.

In a previous study, the ADC values of FNH were reported to vary between 1.75 and 1.49×10^{-3} s/mm².⁶ This can be explained by the high cell density of these lesions.¹⁴ In our study, we determined the mean ADC value of FNH as $1.32 \pm 0.06 \times 10^{-3}$ s/mm². For abscesses, the mean ADC value was previously measured as 0.65×10^{-3} s/mm². This value being similar to malignant lesions is considered to be due to inflammatory cells, bacteria, necrotic tissue, and protein-containing pus within the abscess cavity.¹⁶ In the current study, the mean ADC value of the abscess cavity was found to be $1.28 \pm 0.59 \times 10^{-3}$ s/mm².

In the literature, the mean ADC values of metastases have been reported to range from 0.94 to 1.51×10^{-3} s/mm²,^{6,10,14} while the range for the mean ADC values of HCCs is 0.97 to 1.33×10^{-3} s/mm².^{6,11,14} This has been attributed to the cell density of malignant lesions.¹⁵ In our study, the mean ADC value was observed to be $1.17 \pm 0.10 \times 10^{-3}$ s/mm² for the metastases and $1.28 \pm 0.10 \times 10^{-3}$ s/mm² for the HCCs.

When only ADC values are examined, DWI can significantly differentiate between benign and malignant lesions, while the ADC values of FNH and abscesses are similar to malignant lesions.¹⁶ Necrotic areas in the center of hepatic metastases cause an increase in ADC values, which is comparable to the ADC value of benign lesions.^{5,6,9} In brief, DWI determines cellularity, and therefore FNH, adenomas, and abscesses, which have higher cell density among benign lesions, show diffusion restriction, while cystic necrotic malignant lesions have high ADC values.¹⁷ In the current study, the ADC values of FNH and abscesses were similar to those of malignant lesions.

In all our hemangioma cases, we observed that as the b value on DWI increased, the hemangiomas showed loss of signal, but this was not so pronounced as in cysts, and at higher b values, hemangiomas were still observed as mildly hyperintense compared to the liver. The ADC values of the hemangiomas were also higher compared to the liver parenchyma. These findings led us to consider that a diagnosis of hemangioma can be made by DWI without the need for a contrast-enhanced examination. This assumption should be verified by further studies with larger series.

Cysts show loss of signal at increased b values on DWI due to the free diffusion of water molecules.¹⁷ In our study, as the b values increased in DWIs, the signal intensity of the cysts decreased, and they became isointense to the liver at b1000. This appearance was not observed in the remaining liver lesions. Therefore, we consider that DWI can differentiate between cystic and solid masses.

In a study conducted by Chan et al.¹⁶ the central and peripheral areas of abscesses and necrotic tumors were evaluated separately. The centers of all abscesses showed diffusion restriction,

while the centers of necrotic tumors showed free diffusion. In our study, when the 4 abscess cases were evaluated in the same manner, although all showed low ADC values suggesting malignant masses, the marked peripheral hyperintensity in DWI differentiated the lesions from malignant masses based on iso-hypointensity.

Similar to malignant lesions, FNH also has low ADC values while they are hyperintense on DWI. Therefore, it is not possible to distinguish FNH from malignant masses using DWI.¹⁷ In both of our FNH cases, hyperintensity was observed on DWI, suggesting malignant masses, but the ADC values were low, and thus a benign-malignant differentiation could not be made.

In our study, when we evaluated our cases based on ADC values alone, abscesses were successfully identified when the qualitative evaluation was included in the analysis, increasing the sensitivity value to 100% and specificity to 89%. Therefore, such evaluations should be made both qualitatively and quantitatively.

Limitations

In our study, neither parallel nor respiratory triggered imaging, which are methods to increase image quality, was used. Therefore, the rate of SGO rate was very low. Since only cases with histopathological results were included in the study, the number of our cases was also low. Considering the mass subgroups, we did not have any cases with an adenoma or cystic metastasis.

CONCLUSION

Diffusion-weighted imaging is effective in differentiating benign-malignant liver masses. The evaluation of liver masses with both DWI and ADC values is important for accurate mass characterization, especially for abscesses. Apparent diffusion coefficient values can be used to differentiate cirrhotic and non-cirrhotic livers. Solid cysts, hemangiomas, simple cysts, and hydatid cysts can be differentiated by adding b1000 DWI to the examination. This can facilitate the diagnosis of hemangiomas without using contrast material. Focal nodular hyperplasia imitates malignant lesions in terms of DWI characteristics and ADC value.

Ethics Committee Approval: Ethical committee approval was received from the Ethics Committee of Erciyes University Faculty of Medicine. (Date: March 20, 2009, Decision no: 09/130).

Informed Consent: Written informed consent was obtained from all participants who participated in this study.

Peer-review: Externally peer-reviewed.

Author Contributions: Concept – U.G.O.G, O.I.K.; Design – U.G.O.G, O.I.K.; Supervision – O.I.K.; Resources – U.G.O.G.; Materials – U.G.O.G.; Data Collection – U.G.O.G and/or Processing – U.G.O.G.; Analysis and/or Interpretation – U.G.O.G., Literature Search – U.G.O.G.; Writing Manuscript – U.G.O.G.; Critical Review – O.I.K.

Declaration of Interests: The authors declare that they have no competing interest.

Funding: This study received no funding.

REFERENCES

1. Fujita N, Nishie A, Asayama Y, et al. Hyperintense Liver Masses at hepatobiliary Phase gadoteric acid-enhanced MRI: imaging Appearances and Clinical Importance. *RadioGraphics*. 2020;40(1):72-94. [\[CrossRef\]](#)
2. Tello R, Fenlon HM, Gagliano T, deCarvalho VL, Yucel EK. Prediction rule for characterization of hepatic lesions revealed on MR imaging: estimation of malignancy. *AJR Am J Roentgenol*. 2001;176(4):879-884. [\[CrossRef\]](#)
3. de Figueiredo EH, Borgonovi AF, Doring TM. Basic concepts of MR imaging, diffusion MR imaging, and diffusion tensor imaging. *Magn Reson Imaging Clin N Am*. 2011;19(1):1-22. [\[CrossRef\]](#)
4. Oyar O, Gülsoy UK. *Tıbbi Görüntüleme Fiziği. Suleyman Demirel Üniversitesi Tıp Fakültesi*, 2003;1:281-366.
5. Federau C, Maeder P, O'Brien K, Browaeys P, Meuli R, Hagmann P. Quantitative measurement of brain perfusion with intravoxel incoherent motion MR imaging. *Radiology*. 2012;265(3):874-881. [\[CrossRef\]](#)
6. Chen ZG, Xu L, Zhang SW, Huang Y, Pan RH. Lesion discrimination with breath-hold hepatic diffusion-weighted imaging: a meta-analysis. *World J Gastroenterol*. 2015;21(5):1621-1627. [\[CrossRef\]](#)
7. Miller FH, Hammond N, Siddiqi AJ, et al. Utility of diffusion-weighted MRI in distinguishing benign and malignant hepatic lesions. *J Magn Reson Imaging*. 2010;32(1):138-147. [\[CrossRef\]](#)
8. Lewis S, Dyvorne H, Cui Y, Taouli B. Diffusion-weighted imaging of the liver: techniques and applications. *Magn Reson Imaging Clin N Am*. 2014;22(3):373-395. [\[CrossRef\]](#)
9. Tosun M, Inan N, Sarisoy HT, et al. Diagnostic performance of conventional diffusion weighted imaging and diffusion tensor imaging for the liver fibrosis and inflammation. *Eur J Radiol*. 2013;82(2):203-207. [\[CrossRef\]](#)
10. Testa ML, Chojniak R, Sene LS, et al. Is DWI/ADC a useful tool in the characterization of focal hepatic lesions suspected of malignancy? *PLOS ONE*. 2014;9(7):e101944. [\[CrossRef\]](#)
11. Koh DM, Collins DJ. Diffusion-weighted MR imaging in the body: applications and challenges in oncology. *AJR Am J Roentgenol*. 2007;188(6):1622-1635. [\[CrossRef\]](#)
12. Galea N, Cantisani V, Taouli B. Liver lesion detection and characterization: role of diffusion-weighted imaging. *J Magn Reson Imaging*. 2013;37(6):1260-1276. [\[CrossRef\]](#)
13. Bonekamp S, Corona-Villalobos CP, Kamel IR. Oncologic applications of diffusion-weighted MRI in the body. *J Magn Reson Imaging*. 2012;35(2):257-279. [\[CrossRef\]](#)
14. Wei C, Tan J, Xu L, et al. Differential diagnosis between hepatic metastases and benign focal lesions using DWI with parallel acquisition technique: a meta-analysis. *Tumour Biol*. 2015;36(2):983-990. [\[CrossRef\]](#)
15. Inan N, Arslan A, Akansel G, et al. Diffusion-weighted imaging in the differential diagnosis of simple and hydatid cysts of the liver. *AJR Am J Roentgenol*. 2007;189(5):1031-1036. [\[CrossRef\]](#)
16. Chan JH, Tsui EY, Luk SH, et al. Diffusion-weighted MR imaging of the liver: distinguishing hepatic abscess from cystic or necrotic tumor. *Abdom Imaging*. 2001;26(2):161-165. [\[CrossRef\]](#)
17. Bruegel M, Rummeny EJ. Hepatic metastases use of diffusion-weighted echo-planar imaging. *Abdom Imaging*. 2010;35(4):454-461. [\[CrossRef\]](#)